# PCCP

## PAPER

# Ab initio study of the enantio-selective magnetic-field-induced second harmonic generation in chiral molecules

Antonio Rizzo,*[a] G. L. J. A. Rikken[b] and R. Mathevet[b]

We present a systematic *ab initio* study of enantio-selective magnetic-field-induced second harmonic generation (MFISHG) on a set of chiral systems ((L)-alanine, (L)-arginine and (L)-cysteine; 3,4-dehydro-(L)-proline; (S)-α-phellandrene; (R,S)- and (S,S)-cystine disulphide; N-(4-nitrophenyl)-(S)-prolinol, N-(4-(2-nitrovinyl)-phenyl)-(S)-prolinol, N-(4-tricyanovinyl-phenyl)-(S)-prolinol, (R)-BINOL, (S)-BINAM and 6-(M)-helicene). The needed electronic frequency dependent cubic response calculations are performed within a density functional theory (DFT) approach. A study of the dependence of the property on the choice of electron correlation, on one-electron basis set extension and on the choice of magnetic gauge origin is carried out on a prototype system (twisted oxygen peroxide). The magnetic gauge dependence analysis is extended also to the molecules of the set. An attempt to analyze the structure–property relationships is also made, based on the results obtained for biphenyl (in a frozen twisted conformation), for prolinol and for some of their derivatives. The strength of the effect is discussed, in order to establish its measurability with a proposed experimental setup.

## 1 Introduction

Nonlinear spectroscopies[1–5] are becoming increasingly popular as they are coming out from a small circle of aficionados to reach the communities of researchers working in fields as advanced and strategic as novel (bio)materials, sensors, renewable energy and medical diagnostics. This is due to the rapid advances in laser technology, responding to the growing needs for diverse spectroscopic tools, which could cover regions of spectra where linear spectroscopies are of little use due to lack of transparency of the sample. Multiphoton absorption, MPA, whose theoretical details were unveiled more than eighty years ago, in the early ages of quantum theory, by Göppert-Mayer,[6] and which became a spectroscopic technique after the development of laser sources some fifty years ago,[7,8] is now a full blown area of research and technology, witnessing a unique explosion of interest in the scientific literature and in laboratories everywhere, after having reached much beyond the restricted circles of academy. Coupling the concept of simultaneous absorption of more than one photon with the polarization characteristics of electromagnetic radiation, the ability of light sources to provide

coherent monochromatic highly intense photon fluxes, and combining them in experimental setups where electromagnetic radiation, external generally inhomogeneous fields and matter interact, yields a wide range of possible spectroscopic tools, many still unexplored at the experimental level. Of particular relevance here are the novel spectroscopies addressing chiral molecules, exploiting the different response of enantiomeric configurations.[9–12]

A well known coherent nonlinear process is Second Harmonic Generation (SHG),[1–3,13,14] the non-resonant frequency doubling which has led to major advantages in microscopy,[15] where the virtual absence of photoxidation and self-absorption phenomena and remarkable directionality of SHG have been exploited.[16–20] The dominant light–matter interaction is through electric dipole coupling. Symmetry arguments can be used to show that in the electric dipole approximation, SHG is forbidden in isotropic media, like gases or liquids, and it can be observed only on surfaces, interfaces or locally oriented structures such as membranes[21] or fibrils,[22] where centro-symmetry is permanently broken.

SHG is a special case of the more general process of Sum Frequency Generation,[9,23–26] SFG, exactly as Optical Rectification[27] is a particular example of Difference Frequency Generation.[28] SFG, the absorption of two photons of (different) frequency $\nu_1$ and $\nu_2$, with emission of a single photon of frequency $\nu_1 + \nu_2$ can be observed not only on surfaces and interfaces of locally oriented structures, but also in liquids made of units

[a] *Consiglio Nazionale delle Ricerche – CNR, Istituto per i Processi Chimico-Fisici, UoS di Pisa, Area della Ricerca, Via G. Moruzzi 1, I-56124 Pisa, Italy. E-mail: rizzo@ipcf.cnr.it*

[b] *Laboratoire National des Champs Magnétiques Intenses, UPR3228 CNRS/INSA/UJF/UPS, Toulouse & Grenoble, France*

lacking centro-symmetry, and therefore exhibiting optical activity in the presence of intense electromagnetic radiation. In contrast to other well known linear and nonlinear chiroptical phenomena, which need the involvement of magnetic dipole and/or electric quadrupole interaction to be rationalized, SFG relays entirely on electric dipole interactions.[9,10] The effect disappears in racemic mixtures, and its intensity is proportional to (and it is therefore a measure of) the enantiomeric excess in a solution containing enantiomers.

A static electric field induces SHG in isotropic media, in what is known as Electric-Field-Induced SHG (EFISHG),[29] a phenomenon exploited in electrooptic conversion[1–3,30] and in general in the study of materials. In a recent study,[31] we have analyzed computationally the chiral response of optically active samples in EFISHG experimental setups where circularly polarized radiation is employed,[32] estimating the circular intensity difference (CID) to be observed in yet to be performed experiments involving some representative proteinogenic amino acids. CID is related to what is commonly defined as circular dichroism, CD, the difference in molar extinction for left and right circularly polarized radiation,[11,33] and it yields a tool for the study of stereochemistry and structure of biomolecular conformations.[34–37]

In this paper we will focus our attention on another possible nonlinear process, that is SHG induced by an external static magnetic field, labeled MFISHG, focusing on chiral media. Magnetic field induced SHG has been observed in several instances, in gases,[38] surfaces,[39] solids,[40,41] films and nanoparticles,[42] see also ref. 43 and the theoretical analysis by Kielich and Zawodny,[44] and Manakov and co-workers.[45] Magnetization induced SHG has also been reported,[46] in films,[47] and solids.[48,49] Here we study the case where, as in SFG, the polarization measured after interaction of polarized radiation with a chiral sample, leading to frequency doubling, is different for the distinct enantiomers when the sample is subject to a static magnetic field. The phenomenon has been discussed by Georges H. Wagnière,[4,12] and it is one element of the large variety of high-order optical effects which one can in principle detect in matter by exploiting the high intensity and high coherence of available laser sources. We will focus on the purely electronic form of MFISHG, neglecting orientational effects by the magnetic field. The expression of the macroscopic induced second harmonic generation is related to the microscopic contributions to the frequency dependent induced multipole moments, and in particular to an average taken over appropriate frequency dependent cubic response functions involving electric dipole and magnetic dipole perturbations. The observable is computed for a series of chiral reference systems ((L)-alanine; (L)-arginine; (L)-cysteine; 3,4-dehydro-(L)-proline; (S)-α-phellandrene; (R,S)- and (S,S)-cystine disulphide; N-(4-nitrophenyl)-(S)-prolinol; N-(4-(2-nitrovinyl)-phenyl)-(S)-prolinol; N-(4-tricyanovinyl-phenyl)-(S)-prolinol; (R)-BINOL; (S)-BINAM and 6-(M)-helicene) with the aim of estimating the detectability of the optical effect. For further analysis of the structure–property relationships, and in particular of the effect of donor- and acceptor-substituents on reference molecular frames, calculations were performed on a chiral form of biphenyl, and its derivatives 4-amino-biphenyl,

4-nitro-biphenyl and 4-amino-4′-nitro-biphenyl. A density functional theory time-dependent approach[50,51] has been employed for the response calculations, and a preliminary analysis of the dependence of the observable on some of the critical parameters of these high-order property calculations (electron correlation, choice of the functional, extension and quality of the basis set and, last but not least, dependence of the results on the choice of the magnetic gauge) is carried out on a prototype system, frozen twisted hydrogen peroxide. The dependence of the property on the choice of the origin of the magnetic gauge is also analyzed for the molecules of the set.

In response property calculations involving magnetic dipole interactions the dependence of the results on the choice of the magnetic gauge origin in approximate calculations is often taken care using perturbation-dependent basis sets. Within our group, in particular, we usually resort to Gauge Including Atomic Orbitals (GIAO's, also known as London Atomic orbitals, LAO's).[52] Although cubic response function related properties such as Cotton–Mouton[53] and Jones[54] birefringences have been studied using GIAO's by resorting to the atomic orbital-based response theory allowing for the use of both time- and perturbation-dependent basis sets (OpenRSP approach) pioneered by Ruud and co-workers,[55] those studies employed an independent particle approximation. To our knowledge no implementation of cubic response theory employing electron-correlated structure models is available to date. Note also that only the electronic contributions to the cubic response functions relevant for the observable in the MFISHG experiment are analyzed in this work. Vibrational contributions, which can in principle be non-negligible particularly for some of the molecules included in our set, are not included. Furthermore, our conclusions will apply to isolated, non-interacting molecules, since the effect of the environment is not accounted for.

The layout of the paper follows closely that of ref. 31. In Section 2 the theoretical background is laid down; the computational details are given in Section 3; the results are presented and discussed in Section 4; in Section 5 the experimental setup under construction at the Laboratoire dec Champs Magneétiques Intenses is briefly described and the perspectives for experimental detection of MFISHG are discussed; Section 6 collects our conclusions.

## 2 Theory

### 2.1 Basic formulae

In this section, setting the theoretical background for the study, we will consider the possible symmetry allowed forms that the source terms in Maxwell's equations, like the electric polarization $\mathbf{P}_{2\omega}$ or the magnetization $\mathbf{M}_{2\omega}$, can take, induced by the electric and magnetic field components of an electromagnetic plane wave at frequency $\omega$, $\mathbf{E}_\omega$ and $\mathbf{B}_\omega$ respectively, in the presence of static electric or magnetic fields $\mathbf{E}_0$ and $\mathbf{B}_0$ respectively. In a purely electric dipole approximation, EFISHG is described by

$$\mathbf{P}_{2\omega} = \chi_1(\mathbf{E}_\omega \cdot \mathbf{E}_0)\mathbf{E}_\omega + \chi_2(\mathbf{E}_\omega \cdot \mathbf{E}_\omega)\mathbf{E}_0 \qquad (1)$$

This journal is © the Owner Societies 2016

*Phys. Chem. Chem. Phys.*, 2016, **18**, 1846–1858 | **1847**

with the material parameters $\chi_i$ representing second order hyperpolarizabilities. SHG induced by a static magnetic field is also symmetry allowed, through (to lowest order) the contributions

$$\mathbf{P}_{2\omega} = \chi_1(\mathbf{B}_\omega \cdot \mathbf{B}_0)\mathbf{E}_\omega + \chi_2(\mathbf{E}_\omega \cdot \mathbf{B}_0)\mathbf{B}_\omega \qquad (2)$$

and

$$\mathbf{M}_{2\omega} = \zeta_1(\mathbf{E}_\omega \cdot \mathbf{B}_0)\mathbf{E}_\omega + \zeta_2(\mathbf{E}_\omega \cdot \mathbf{E}_\omega)\mathbf{B}_0 \qquad (3)$$

These effects (observable in principle in all media) involve more than one magnetic dipole interaction and therefore are very weak. They are generally neglected, but have been experimentally observed.[38] If the medium is chiral, that is if $\chi_i^D = -\chi_i^L$, and we are looking for optical electric dipole interactions to generate MFISHG, the only symmetry allowed form is

$$\mathbf{P}_{2\omega} = \psi_1^{D/L}\left(\frac{\partial \mathbf{E}_\omega}{\partial t} \cdot \mathbf{B}_0\right)\mathbf{E}_\omega + \psi_2^{D/L}\left(\frac{\partial \mathbf{E}_\omega}{\partial t} \cdot \mathbf{E}_\omega\right)\mathbf{B}_0 \qquad (4)$$

which for a harmonic electromagnetic field can be written as

$$\mathbf{P}_{2\omega} = i\omega\psi_1^{D/L}(\mathbf{E}_\omega \cdot \mathbf{B}_0)\mathbf{E}_\omega + i\omega\psi_2^{D/L}(\mathbf{E}_\omega \cdot \mathbf{E}_\omega)\mathbf{B}_0 \qquad (5)$$

The intuitive physical interpretation of eqn (1) is that the polar character of the medium, induced by the external electric field, distorts its response to the alternating electric field, generating even harmonics. A similarly intuitive physical picture behind eqn (4) can be found by realizing that

$$\frac{\partial}{\partial t}\mathbf{E}_\omega = \frac{1}{\chi}\frac{\partial}{\partial t}\mathbf{P}_\omega = \frac{1}{\chi}\mathbf{I}_\omega \qquad (6)$$

$\mathbf{I}_\omega$ being the induced current density at optical frequencies and $\chi$ the electrical susceptibility. We can then write

$$\mathbf{P}_{2\omega} = \frac{\psi_1^{D/L}}{\chi}(\mathbf{I}_\omega \cdot \mathbf{B}_0)\mathbf{E}_\omega \qquad (7)$$

The medium response is therefore different whether the induced current is parallel or anti-parallel to the external magnetic field. Such an effect has already been observed at low frequencies[56–59] and was called electrical magneto-chiral anisotropy (eMChA). SHG induced by a static magnetic field in chiral media can therefore be described as the result of eMChA at optical frequencies.

A possible setup for the experiment discussed theoretically above is schematized in Fig. 1. A linearly polarized electromagnetic beam impinges in a fluid made by noninteracting, chiral molecule subject also to a static external magnetic induction field $\mathbf{B}_0$ with a component aligned parallel to the direction of polarization of radiation. In the setup of Fig. 1, two photons
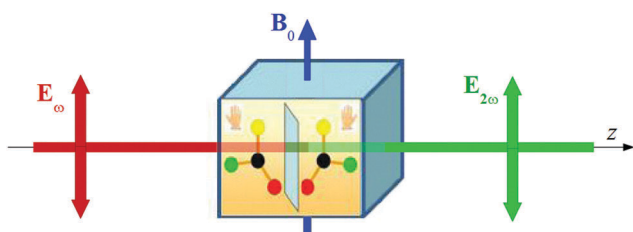


Fig. 1   Schematic setup of the MFISHG experiment.

of circular frequency $\omega$ are absorbed and a photon with circular frequency equal to $2\omega$ is emitted, in a process that we call, in analogy with its electric field a far more popular counterpart, MFISHG, magnetic field induced second harmonic generation. As recognized by Wagnière,[4,12] the process, a particular example of the more general phenomenon of magnetic field induced sum frequency generation, involves the mixed electric and magnetic nonlinear optical response of the sample. In particular, focusing on third order effects, the average electric dipole moment $\mathbf{p}_{2\omega}$ induced in a molecule by the interaction with the electromagnetic radiation in the static magnetic field, $\mathbf{p}_{2\omega} = \mathbf{p}^{(3)}(-2\omega;\omega,\omega,0)$, a vector, can be written as

$$\mathbf{p}^{(3)}(-2\omega;\omega,\omega,0) = 2i\langle\chi'^{(3)}(-2\omega;\omega,\omega,0)\rangle(\mathbf{E}_\omega \cdot \mathbf{B}_0)\mathbf{E}_\omega \qquad (8)$$

Here $\chi'^{(3)}(-2\omega;\omega,\omega,0)$ is the third order molecular susceptibility tensor of rank four.[2–5] The brackets indicate an isotropical average needed in fluids, yielding a scalar or, as in the specific case discussed here, a pseudoscalar. The three field vectors involved in the process are combined (a scalar product of two of them multiplied by the third) in order to yield a vector. The particular sequence of field vectors chosen in eqn (8) stands for any of the possible permutations. The third order susceptibility, formally represented by the label $m'\mu\mu\mu$ by Wagnière in ref. 4 and 12, after proper spatial averaging, carried out using the approach and expressions listed in ref. 4, 12 and 60, can be written as

$$\left\langle \chi'^{(3)}(-2\omega;\omega,\omega,0) \right\rangle$$

$$= +\frac{1}{5}\xi_{X,X,X,X}^{\omega,\omega,0} + \frac{1}{5}\xi_{Y,Y,Y,Y}^{\omega,\omega,0} + \frac{1}{5}\xi_{Z,Z,Z,Z}^{\omega,\omega,0} + \frac{2}{15}\xi_{X,X,Y,Y}^{\omega,\omega,0} + \frac{2}{15}\xi_{X,X,Z,Z}^{\omega,\omega,0}$$

$$+ \frac{2}{15}\xi_{Y,Y,X,X}^{\omega,\omega,0} + \frac{2}{15}\xi_{Y,Y,Z,Z}^{\omega,\omega,0} + \frac{2}{15}\xi_{Z,Z,X,X}^{\omega,\omega,0} + \frac{2}{15}\xi_{Z,Z,Y,Y}^{\omega,\omega,0} + \frac{1}{15}\xi_{X,Y,Y,X}^{\omega,\omega,0}$$

$$+ \frac{1}{15}\xi_{X,Z,Z,X}^{\omega,\omega,0} + \frac{1}{15}\xi_{Y,X,X,Y}^{\omega,\omega,0} + \frac{1}{15}\xi_{Y,Z,Z,Y}^{\omega,\omega,0} + \frac{1}{15}\xi_{Z,X,X,Z}^{\omega,\omega,0} + \frac{1}{15}\xi_{Z,Y,Y,Z}^{\omega,\omega,0}$$

$$(9)$$

where

$$\xi_{\alpha,\beta,\gamma,\delta}^{\omega,\omega,0} = \xi_{\alpha,\beta,\gamma,\delta}(-2\omega;\omega,\omega,0) = -i\langle\langle \mu_\alpha;\mu_\beta,\mu_\gamma,m_\delta \rangle\rangle_{\omega,\omega,0} \qquad (10)$$

indicates a frequency dependent cubic response function involving the electric dipole operator $\mu$

$$\mu = \sum_j q_j\mathbf{r}_j$$

and the magnetic dipole operator $\mathbf{m}$

$$\mathbf{m} = \sum_j \frac{q_j}{2M_j}(\mathbf{r}_j \times \mathbf{p}_j) = \sum_j \frac{q_j}{2M_j}\mathbf{l}_j. \qquad (11)$$

Above the charge $q_j$, the spatial coordinate $\mathbf{r}_j$, the masses $M_j$, the linear momentum $\mathbf{p}_i = -i\hbar\nabla_i$ and the orbital angular momentum $\mathbf{l}_j = (\mathbf{r}_j \times \mathbf{p}_j)$ of particle $j$ are introduced. The cubic response in eqn (10) is an axial (parity) odd (time reversality) tensor of fourth order, and the effect, according to ref. 61, occurs only in a medium of non-centrosymmetric molecules. Moreover,

the following permutation symmetry relationships apply when all frequencies are far away from molecular resonances

$$\xi_{\alpha,\beta,\gamma,\delta}(-2\omega;\omega,\omega,0) = \xi_{\alpha,\beta,\delta,\gamma}(-2\omega;\omega,0,\omega) = \xi_{\alpha,\delta,\gamma,\beta}(-2\omega;0,\omega,\omega) \tag{12}$$

which imply

$$\langle \chi'^{(3)}(-2\omega;\omega,\omega,0) \rangle = \omega \psi_1^{D/L} = \omega \psi_2^{D/L}$$

For a general discussion of nonlinear susceptibilities and their sum-over-state representation the reader should refer to the textbook ref. 2–5, see also ref. 62. Frequency dependent cubic response functions as those represented in eqn (10) can be obtained nowadays resorting to a fully analytical approach developed about thirty years ago,[63,64] and that avoids the recourse to approximate sum-over-state schemes. The approach was applied to a wide range of electronic structure models, as SCF[65] and MCSCF,[66] Coupled Cluster[67] and DFT.[68,69] In this study we resort to the latter to obtain an estimate of the the polarization described by eqn (8).

## 2.2 Origin dependence

When the origin of the multipolar expansion is displaced from **O** to **O**′, say **O**′ = **O** + **R**, which implies that the transformation **r**′ = **r** − **R**, the operators $\mu$ and $m$, in a neutral system, are transformed as follows $\Delta Y_i = Y_i' - Y_i, i = x, y, z$[36]

$$\Delta \mu_i = 0 \tag{13}$$

$$\Delta m_i = -\frac{1}{2}\varepsilon_{i\alpha\beta}R_\alpha \mu_\beta^p \tag{14}$$

where $\mu^p$ is the velocity operator

$$\mu^p = \sum_j \frac{q_j}{M_j}\mathbf{p}_j$$

These relationships can be used to derive an expression for the change in the response function tensor elements of eqn (10)

$$\xi_{\alpha,\beta,\gamma,\delta}^{\omega,\omega,0}(\mathbf{O}') = \xi_{\alpha,\beta,\gamma,\delta}^{\omega,\omega,0}(\mathbf{O}) + \frac{1}{2}\varepsilon_{\delta\rho\sigma}R_\rho \nu_{\alpha,\beta,\gamma,\sigma}^{\omega,\omega,0} \tag{15}$$

where

$$\nu_{\alpha,\beta,\gamma,\delta}^{\omega,\omega,0} = \nu_{\alpha,\beta,\gamma,\delta}(-2\omega;\omega,\omega,0) = +i \langle\!\langle \mu_\alpha; \mu_\beta, \mu_\gamma, \mu_\delta^p \rangle\!\rangle_{\omega,\omega,0}. \tag{16}$$

and $\varepsilon_{\alpha\beta\gamma}$ is the alternating Levi-Civita tensor. In the limit a complete one-electron basis set, the hypervirial relationship

$$[\mu_\alpha, \mathcal{H}] = i\mu_\alpha^p \tag{17}$$

holds, and we can exploit the equations of motions holding for exact cubic response functions,[63,64]

$$(\omega_1 + \omega_2 + \omega_3 + 3i\varepsilon)\langle\!\langle V^{\omega_0}; V^{\omega_1}, V^{\omega_2}, V^{\omega_3} \rangle\!\rangle_{\omega_1,\omega_2,\omega_3}$$

$$= \langle\!\langle [V^{\omega_0}, \mathcal{H}]; V^{\omega_1}, V^{\omega_2}, V^{\omega_3} \rangle\!\rangle_{\omega_1,\omega_2,\omega_3}$$

$$+ \frac{1}{2}\mathcal{P}_{123}\langle\!\langle V^{\omega_0}, V^{\omega_1}; V^{\omega_2}, V^{\omega_3} \rangle\!\rangle_{\omega_2,\omega_3} \tag{18}$$

where $V^\omega$ denotes the perturbation of circular frequency $\omega$, $\mathcal{H}$ is the Hamiltonian, $\mathcal{P}_{i,j,...}$ indicates all permutations of the

indices $i, j, ...$ The combination of eqn (17) and (18) allows us to prove that, for the "exact" case, or (equivalently) in the limit of a complete one-electron basis set,

$$\nu_{\alpha,\beta,\gamma,\delta}^{\omega,\omega,0} \to 0 \tag{19}$$

In approximate calculations, on the other hand, the third order susceptibility tensor at the displaced origin can be written as

$$\langle \chi'^{(3)}(-2\omega;\omega,\omega,0) \rangle(\mathbf{O}') = \langle \chi'^{(3)}(-2\omega;\omega,\omega,0) \rangle(\mathbf{O}) + \mathbf{R}\cdot\mathbf{S} \tag{20}$$

where

$S_X$

$$= -\frac{1}{15}\nu_{X,Y,X,Z}^{\omega,\omega,0} + \frac{1}{15}\nu_{X,Z,X,Y}^{\omega,\omega,0} - \frac{1}{30}\nu_{Y,X,X,Z}^{\omega,\omega,0} - \frac{1}{10}\nu_{Y,Y,Y,Z}^{\omega,\omega,0} + \frac{1}{15}\nu_{Y,Z,Y,Y}^{\omega,\omega,0}$$

$$- \frac{1}{30}\nu_{Y,Z,Z,Z}^{\omega,\omega,0} + \frac{1}{30}\nu_{Z,X,X,Y}^{\omega,\omega,0} + \frac{1}{30}\nu_{Z,Y,Y,Y}^{\omega,\omega,0} - \frac{1}{15}\nu_{Z,Z,Y,Z}^{\omega,\omega,0} + \frac{1}{10}\nu_{Z,Z,Z,Y}^{\omega,\omega,0} \tag{21}$$

$S_Y$

$$= \frac{1}{10}\nu_{X,X,X,Z}^{\omega,\omega,0} + \frac{1}{30}\nu_{X,Y,Y,Z}^{\omega,\omega,0} - \frac{1}{15}\nu_{X,Z,X,X}^{\omega,\omega,0} + \frac{1}{30}\nu_{X,Z,Z,Z}^{\omega,\omega,0} + \frac{1}{15}\nu_{Y,Y,X,Z}^{\omega,\omega,0}$$

$$- \frac{1}{15}\nu_{Y,Z,Y,X}^{\omega,\omega,0} - \frac{1}{30}\nu_{Z,X,X,X}^{\omega,\omega,0} - \frac{1}{30}\nu_{Z,Y,Y,X}^{\omega,\omega,0} + \frac{1}{15}\nu_{Z,Z,X,Z}^{\omega,\omega,0} - \frac{1}{10}\nu_{Z,Z,Z,X}^{\omega,\omega,0} \tag{22}$$

$S_Z$

$$= -\frac{1}{10}\nu_{X,X,X,Y}^{\omega,\omega,0} + \frac{1}{15}\nu_{X,Y,X,X}^{\omega,\omega,0} - \frac{1}{30}\nu_{X,Y,Y,Y}^{\omega,\omega,0} - \frac{1}{30}\nu_{X,Z,Z,Y}^{\omega,\omega,0} + \frac{1}{30}\nu_{Y,X,X,X}^{\omega,\omega,0}$$

$$- \frac{1}{15}\nu_{Y,Y,X,Y}^{\omega,\omega,0} + \frac{1}{10}\nu_{Y,Y,Y,X}^{\omega,\omega,0} + \frac{1}{30}\nu_{Y,Z,Z,X}^{\omega,\omega,0} - \frac{1}{15}\nu_{Z,Z,X,Y}^{\omega,\omega,0} + \frac{1}{15}\nu_{Z,Z,Y,X}^{\omega,\omega,0} \tag{23}$$

## 3 Computational details

This exploratory study was carried out on a set of optically active molecular systems whose structures are shown in Fig. 2. The set includes: three proteinogenic amino acids ((L)-alanine, (L)-arginine and (L)-cysteine); five molecules—3,4-dehydro-(L)-proline, (S)-α-phellandrene, (R,S)- and (S,S)-cystine disulphide and N-(4-nitrophenyl)-(S)-prolinol, considered as typical prototypes of chiral systems with remarkable linear and nonlinear optical responses; two bi-aryls (1-1′-bi-2-R-naphtol—(R)-BINOL and (S)-1-1′-binaphtalene-2-2′-diamine—(S)-BINAM) and an helicene (6-(M)-helicene). In order to analyze the relationship between the structure and property, and in particular the effect of electron-donating and electron-withdrawing substituents on reference scaffolds, two non-commercially available derivatives of N-(4-nitrophenyl)-(S)-prolinol (N-(4-(2-nitrovinyl)-phenyl)-(S)-prolinol and N-(4-tricyanovinyl-phenyl)-(S)-prolinol), and four model systems as a frozen twisted conformation of (R)-biphenyl and its (R)-4-amino-biphenyl, (R)-4-nitro-biphenyl
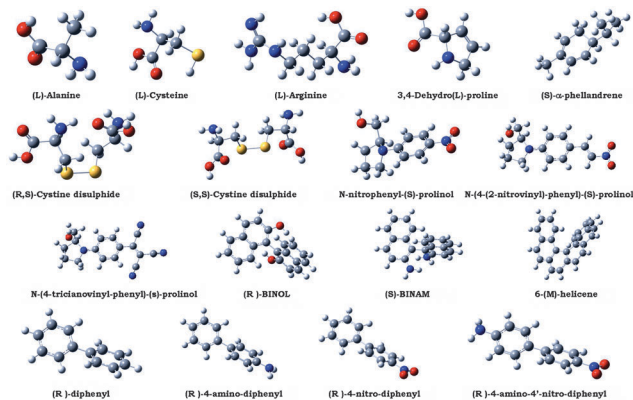
This journal is © the Owner Societies 2016

Phys. Chem. Chem. Phys., 2016, **18**, 1846–1858 | **1849**

Fig. 2  The test set of molecules employed in the exploratory *ab initio* study.

and (*R*)-4-amino-4′-nitro-biphenyl derivatives were also studied. Structures were optimized in the gas phase. For the three proteinogenic amino acids and for (*R*)-BINOL the geometries optimized at the B3LYP/6-31g(d,p) level[70–73] and already employed in ref. 31 and 74 were adopted. The structure of (*R*)-BINOL is taken from the study carried out by Sahnoun and co-workers.[75] The structure of 6-(*M*)-helicene was the one optimized at the B3LYP/6-31G*[76] level already employed in ref. 77. The geometrical parameters of all remaining molecules were optimized in this work at the B3LYP/aug-cc-pVTZ[78,79] level using Gaussian.[80]

The calculation of the frequency dependent cubic response function tensor components was carried out for the isolated molecules at the TD-DFT level,[50,51] employing the B3LYP functional[70–72] with the aug-cc-pVTZ basis set.[78,79] We exploited the development of a quadratic and cubic response beyond the adiabatic local density approximation,[68] implemented in the dalton code.[81,82] The wave length was chosen to be $\lambda$ = 1064 nm for all molecules. For (L)-alanine and (*R*)-BINOL calculations were performed also at $\lambda$ = 780.8 nm and $\lambda$ = 632.8 nm, to analyze the wavelength dependence of the property. In the calculations the center of nuclear masses was adopted as the origin of the magnetic gauge. The threshold for the iterative solution of the linear response equations was set to $10^{-6}$.

For this preliminary analysis we performed a study of the dependence of the property on the quality and extension of the basis set, on the choice of the particular density functional and on the choice of origin of the magnetic gauge focusing on a test system. Following the scheme adopted for the study of the electric field induced SHG circular intensity difference of ref. 31, see also ref. 83, we concentrated our attention on a chiral form of hydrogen peroxide ($H_2O_2$), taken at the geometry adopted in ref. 31 and 83 ($R_{O-O}$ = 1.48 Å, $R_{O-H}$ = 0.95 Å, OÔH = 109.47° and HÔOH = 120°). The hierarchy of augmented correlation consistent basis sets x-aug-ccpVXZ (x = −, d, t, q; X = D, T, Q, 5; stopping at x = d within the 5Z family)[78] was employed for the basis set and choice of magnetic gauge origin studies. The $S_z$ vector component, see eqn (20) and (23) above, was computed for a shift of the origin from the center of nuclear masses along the inter-oxygen direction (the $S_x$ and $S_y$ components vanish for any arbitrary translation of the origin **R**).

Table 1  The third order susceptibility $\langle \chi'^{(3)}(-2\omega;\omega,\omega,0) \rangle$. $\lambda$ = 1064 nm. B3LYP/aug-cc-pVTZ

| System | $\langle \chi'^{(3)}(-2\omega;\omega,\omega,0) \rangle$/a.u. |
|---|---|
| (L)-Alanine | −0.3767 |
| (L)-Cysteine | −0.5203 |
| (L)-Arginine | 0.2748 |
| 3,4-Dehydro-(L)-proline | 1.893 |
| (*S*)-α-Phellandrene | −7.387 |
| (*R*,*S*)-Cystine disulfide | −2.597 |
| (*S*,*S*)-Cystine disulfide | 7.740 |
| *N*-(Nitrophenyl)-(*S*)-prolinol | 13.20 |
| *N*-(4-(2-Nitrovinyl)-phenyl)-(*S*)-prolinol | 6.452 |
| *N*-(4-Tricyanovinyl-phenyl)-(*S*)-prolinol | −38.76 |
| (*R*)-BINOL | −16.61[a] |
| (*S*)-BINAM | 23.82 |
| 6-(*M*)-Helicene | 96.49 |
| (*R*)-Biphenyl | 5.675 |
| (*R*)-4-Amino-biphenyl | 7.849 |
| (*R*)-4-Nitro-biphenyl | −20.54 |
| (*R*)-4-Amino-4′-nitro-biphenyl | −135.2 |

[a] At $\lambda$ = 780 nm, $\langle \chi'^{(3)}(-2\omega;\omega,\omega,0) \rangle$ = −120.0 a.u. At $\lambda$ = 632.8 nm, which in our case means less than 5 nm away from the 2-photon intermediate state resonance with the third excited state, $\langle \chi'^{(3)}(-2\omega;\omega,\omega,0) \rangle$ = −3703 a.u.

The study of the dependence on the choice of density functional was carried out using the d-aug-cc-pV5Z basis set and resorting, in addition to B3LYP, to four other popular functionals: BLYP,[71,72,84] BHandHLYP,[85] Cam-B3LYP,[86–88] and SVWN5.[89] BLYP[71,72,84] combines Becke's 1988 functional[71]—including both Slater's exchange[90] and corrections involving the gradient of the density—with both local and non-local terms of Lee, Yang, and Parr's correlation functional.[72,84] The Half-and-half Functional BHandHLYP[85] employs an equal fraction of Hartree–Fock, Local Spin Density Approximation (LSDA)[89] and Becke 88 exchange[71] together with the LYP correlation contribution.[72,84] CAM-B3LYP[86–88] is a long range corrected version of B3LYP where the Coulomb-attenuating method was employed. SVWN5[89] couples the Slater exchange functional[90] with the Volko, Wilk and Nussair correlation functional, and it is equivalent to LSDA.

# 4 Results and discussion of calculations

The results obtained for the third order susceptibility $\langle \chi'^{(3)}(-2\omega;\omega,\omega,0) \rangle$ at the wavelength $\lambda$ = 1064 nm are shown in Table 1.

Among the chosen proteinogenic acids, (L)-cysteine yields the strongest response at $\lambda$ = 1064 nm, twice as strong as that of (L)-arginine and about 35% stronger than (L)-alanine (absolute values). For the latter, note that as we perform the calculation at shorter wavelengths, see Table 2, the third order susceptibility increases, with a strong enhancement, by a factor of twenty, at $\lambda$ = 632.8 nm ($\approx$1.95 eV, that is more than 1 eV lower than needed to approach the two-photon resonance with the first excited state, placed at $\approx$5.96 eV[91]). We will come back to the phenomenon of near resonant enhancement later on. Here we note that the observable appears to be, at least in the cases we analyzed, quite sensitive to the change in circular frequency.

view of the distribution of the lowest four excited states of the molecules included in an analysis, as obtained at the B3LYP/aug-cc-pVTZ level, and it shows where the one-photon and two-photon resonances lie in the energy spectrum when the three laser wavelengths (1064 nm, 780 nm and 632.8 nm) are considered. The seventeen systems listed in Table 1 are identified in the figure by acronyms, and are arranged in the same order as in the table. The lowest excited state of (N-(4-tricyanovinyl-phenyl)-(S)-prolinol) (TCVPP in the figure) is placed at 2.87 eV ($\lambda$ = 431.6 nm), *ca.* 100 nm off the two-photon resonance at an electromagnetic field wavelength of 1064 nm. This near resonance has most likely a relevant effect on the quite strong response of (N-(4-tricyanovinyl-phenyl)-(S)-prolinol) $\langle \chi'^{(3)}(-2\omega;\omega,\omega,0) \rangle \approx -39$ a.u., see above and Table 1. Rather obviously, as the circular frequency of radiation increases, the probability of meeting the conditions of resonance increases. Apparently, two-photon near resonant conditions are met for the lowest state of N-(4-(2-nitrovinyl)-phenyl)-(S)-prolinol, NVPP in the figure ($\lambda$ = 387.2 nm), for the lowest two near degenerate states of 6-(M)-helicene ($\lambda_1$ = 388 nm, $\lambda_2$ = 371 nm) and for (R)-4-amino-4′-nitro-biphenyl, ANDph in the figure, $\lambda$ = 397 nm. The two-photon resonances corresponding to radiation impinging at $\lambda$ = 632.8 are numerous throughout the set molecules placed in the second half of Table 1.
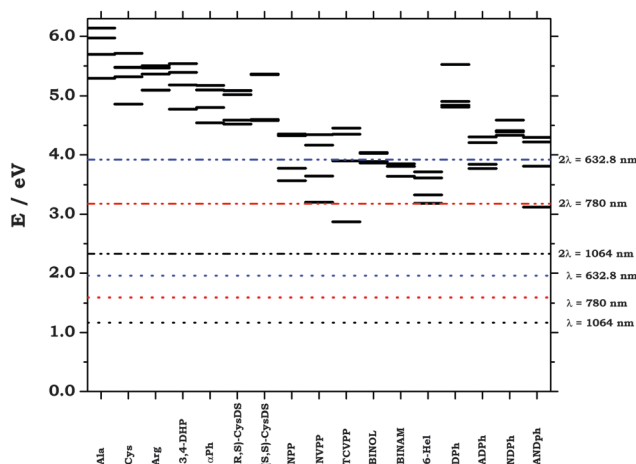
If the value computed for the third order susceptibility for (R)-BINOL at $\lambda$ = 632.8 nm is clearly dictated by the evidence that the lowest four excitation energies are clustered within 26 nm around half the laser wavelength, near two-photon resonant conditions cannot explain (at least not alone) the remarkable enhancement (by a factor of seven, from $\approx -17$ a.u. to $\approx -120$ a.u.) seen for the same biaryl when going from $\lambda$ = 1064 nm to $\lambda$ = 780 nm. Our lowest-order perturbation theory approach is obviously inadequate to treat resonant conditions in two-photon theory. These that can be better (albeit still approximately, in as much as it resorts to the use of phenomenological damping parameters) handled by damped response theory, as introduced by Norman and co-workers[94,95] and later by Kristensen and co-workers[96] in a formulation that was recently employed in a study of two-photon absorption involving one of the present authors.[97] To our knowledge, an appropriate damped response code that could handle cubic response properties is still missing.

## 4.2 Magnetic gauge origin dependence

In order to estimate the dependence of the property under analysis in this study on the choice of the magnetic field gauge we computed the vector **S**, defined in eqn (20), see also eqn (21) to (23), at the B3LYP/aug-cc-pVTZ level, for $\lambda$ = 1064 nm, for the seventeen molecules of our set. Table 4 collects the results.

In order to give a rough estimate of the effect of a change in the magnetic gauge origin on a given molecule, we use the percentage change (in absolute value) of the MFISHG listed in Table 1 upon displacement of the magnetic gauge origin by a vector **R** = (10., 10., 10.) a.u. (last column in Table 4). In most cases such displacement changes the property by less than 10%. Exceptions are the proteinogenic acids, exhibiting a relatively weak MFISHG, which can change by up to more than 30% upon the given change of origin, and the two derivatives of N-(nitrophenyl)-prolinol, where N-(4-(2-nitrovinyl)-phenyl)-(S)-prolinol (in particular) has a strong response to the displacement of origin, by $\approx 68\%$, mostly due to the large value of $S_y$. The $y$ axis goes perpendicular to the plane defined by the pyrolidine nitrogen and its two carbon neighbors and the (slightly tilted) plane of the phenyl ring and its nitrovinyl substituent. It is therefore nearly aligned to the C–C bond connecting the methanol group and the five membered ring. The MFISHG of N-(4-tricyanovinyl-phenyl)-(S)-prolinol is also quite sensitive to the change in the magnetic gauge origin, with quite large contributions coming again from $S_y$. The results in this section, if compared to the conclusions of the study on the model study on frozen twisted hydrogen peroxide given in the Appendix, show that the dependence of the spatially averaged third order susceptibility contributing to MFISHG on the choice of the magnetic gauge origin is less severe on large, extended molecules than on small systems.

**Table 4** The **S** vector (units o $10^2 \times$ a.u.). $\lambda$ = 1064 nm. B3LYP/aug–cc–pVTZ. In the last column, the percentage change of the property (*cf.* Table 1) for a change in the origin through the vector **R** = (10., 10., 10.) a.u. is given

| System | $S_x$ | $S_y$ | $S_z$ | Perc. |
|---|---|---|---|---|
| (L)-Alanine | −1.0065 | 0.4232 | −0.6289 | 32.2 |
| (L)-Cysteine | 0.1186 | 1.9041 | −0.8274 | −23.0 |
| (L)-Arginine | −0.0242 | 0.3184 | −1.1422 | −30.9 |
| 3,4-Dehydro-(L)-proline | 3.4266 | 0.1222 | −2.2863 | 6.7 |
| (S)-α-Phellandrene | 3.4266 | 0.1222 | −2.2863 | −1.7 |
| (R,S)-Cystine disulfide | −1.3570 | −1.2926 | −0.4861 | 12.1 |
| (S,S)-Cystine disulfide | 3.1612 | 2.4226 | 2.2542 | 10.1 |
| N-(Nitrophenyl)-(S)-prolinol | −2.8542 | 10.5977 | 6.5689 | 10.8 |
| N-(4-(2-Nitrovinyl)-phenyl)-(S)-prolinol | −9.7302 | −48.8993 | 14.5598 | −68.3 |
| N-(4-Tricyanovinyl-phenyl)-(S)-prolinol | −13.6794 | 95.3782 | 9.8342 | −23.6 |
| (R)-BINOL | 0.0000 | 0.0000 | −6.4878 | 3.9 |
| (S)-BINAM | 5.1076 | −2.3164 | 4.4359 | 3.0 |
| 6-(M)-Helicene | −0.0026 | −26.3366 | 0.0059 | −2.7 |
| (R)-Biphenyl | 0.0017 | −0.0075 | 0.0048 | 0.0 |
| (R)-4-Amino-biphenyl | −0.2180 | 10.9710 | 15.3791 | −12.7 |
| (R)-4-Nitro-biphenyl | −2.9692 | −0.0031 | −0.0028 | −3.8 |
| (R)-4-Amino-4′-nitro-biphenyl | −5.6079 | −6.8277 | 34.2538 | −1.6 |

**1852** | *Phys. Chem. Chem. Phys.,* 2016, **18**, 1846–1858

This journal is © the Owner Societies 2016

# 5 Experimental perspectives

The relation between the dipole moment in SI units and the third order susceptibility in atomic units is[98]

$$\mathbf{p}^{(3)}(-2\omega;\omega,\omega,0) \; [\text{C m}] = 1.36411 \times 10^{-58} \times \langle \chi'^{(3)}(-2\omega;\omega,\omega,0) \rangle$$
$$[\text{a.u.}] \times (\mathbf{E} \; [\text{V m}^{-1}])^2 \times (\mathbf{B} \; [\text{T}]) \tag{24}$$

Above we specify within square brackets the units for the associated quantity. In SI units, bulk SHG is usually described by

$$\mathbf{P}_{\text{SHG}}(-2\omega;\omega,\omega,0) \equiv \varepsilon_0 \mathbf{d}{:}{:}\mathbf{E}_\omega \mathbf{E}_\omega \tag{25}$$

where $\mathbf{d}$ is the SHG tensor (units m V$^{-1}$). We define similarly the MFISHG tensor $\tilde{\mathbf{d}}$

$$\mathbf{P}_{\text{MFISHG}}(-2\omega;\omega,\omega,0) \equiv \varepsilon_0 \tilde{\mathbf{d}}{:}{:}{:}\mathbf{B}_0 \mathbf{E}_\omega \mathbf{E}_\omega \tag{26}$$

(units m V$^{-1}$ T$^{-1}$). Combining eqn (25) and (26) leads to

$$\tilde{\mathbf{d}} = 1.54064 \times 10^{-47} \langle \chi'^{(3)} \rangle N \tag{27}$$

where $N$ is the molecular density (units m$^{-3}$). In order to determine the measurability of MFISHG, we should compare $\tilde{\mathbf{d}}\mathbf{B}_0$ with the detection limits for the SHG tensor components $\mathbf{d}$. If we deliberately focus on non-resonant conditions, and consider the calculated result for (R)-BINOL at $\lambda = 780$ nm, at a concentration of 10 molar, and a magnetic field of 30 T, we find $\tilde{\mathbf{d}}\mathbf{B}_0 = 0.55$ fm V$^{-1}$. Experimental values of $\mathbf{d} = 3.3$ fm V$^{-1}$ have been reported (e.g. $\mathbf{d}_{32}$ of potassium pentaborate),[99] implying that a dedicated effort is necessary to observe MFISHG.

The MFISHG electric field $\mathbf{E}_{\text{MFISHG}}(2\omega)$ is proportional to $\tilde{\mathbf{d}}$. As $\tilde{\mathbf{d}}^D = -\tilde{\mathbf{d}}^L$, electric fields from samples with opposite handedness are opposite, but the measured intensities, proportional to $\mathbf{E}_{\text{MFISHG}}{}^2$, are equal. To recover the opposite signs of the MFISHG electric fields of the two enantiomers, one can let this MFISHG optical wave interfere with a SHG wave of similar amplitude generated in a separate SGH crystal positioned in the fundamental beam just behind the chiral sample being studied. The amplitude of the summed SHG wave will become dependent on the handedness of the sample. The setup under construction for the experimental observation of MFISHG is shown in Fig. 4. It consists of a Chameleon Ultra II Ti-sapphire oscillator (Coherent, Inc.) with tunable wavelength between 680 nm and 1080 nm delivering 140 fs pulse at a repetition frequency of 80 MHz. At optimal wavelengths (780–800 nm) average power is above 3.5 W which corresponds to a peak power above 300 kW. Assuming slight focusing down to a beam waist of 50 μm which corresponds to a 10 mm Rayleigh range, the maximum electric field is on the order of 240 MV m$^{-1}$ which exceeds the dielectric strength of most organic solvents.

The magnetic field will be generated by a split coil magnet inspired by ref. 100 generating slightly under damped pulses ($Q \sim 3$–4 ideally suited for better signal extraction), in a typical (5 mm)$^3$ volume with 1 ms oscillation time and 40 T maximum amplitude at a repetition rate of 1 per 30 minutes. With appropriate overall downsizing and optimized forced cooling, one 30 T shot per few minutes can be achieved.
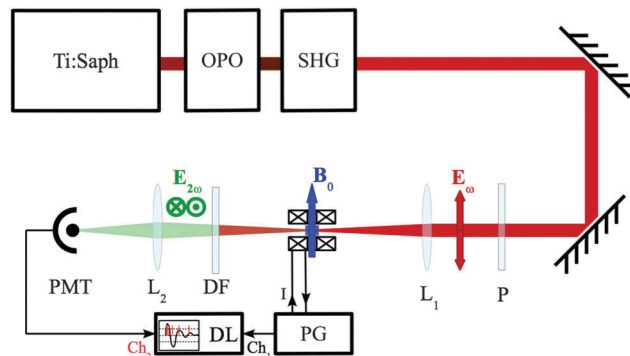


Fig. 4 Experimental setup. Ti:Saph: master oscillator (45 nJ, 140 fs pulses at 80 MHz), OPO: optical parametric oscillator (optional), SHG: second harmonic generator (optional), P: polarizer, L$_{1,2}$: lenses, DF: dichroic filter, PM: photomultiplier, PG: current pulse generator, DL: data logger. $\mathbf{B}_0$: 30 T, 1 ms magnetic field pulse perpendicular to light incident polarization $\mathbf{E}_\omega$.

# 6 Conclusions

The observable (the MFISHG third order susceptibility) is, as already seen for other high order frequency dependent properties arising from the interaction of molecules with electric and magnetic multipoles, computationally highly demanding. It shows a non-negligible dependence on all the variables involved, particularly relevant when it comes to electron correlation, the choice of the form of the functional in the TD-DFT approximation and the choice of the magnetic gauge. Further analysis is needed, and the exploitation of novel developments in the area of computational chemistry, as the use of sophisticated electron correlated structure models (as coupled cluster in its CC2 declination, which can nowadays be employed for robust predictions of mixed electric and magnetic properties, see for example ref. 101), and gauge origin invariant approaches, or of the forthcoming new high response methodologies, exploiting linear scaling techniques, or within the quantum mechanics/molecular mechanics framework. Also, the effect of the environment and of molecular vibrations should be taken into account, which further complicates the picture. The results obtained for MFISHG suggest that this effect is at the limits of measurability. A systematic study of structure–property relationships may identify molecules exhibiting a MFISHG effect falling within current experimental reach.

The MFISHG effect, that can appear in electrically conducting materials, such as ionic solutions, conducting polymers and others, is predicted to be very small, at the limit of detectability indeed. As such, it cannot be suggested as a tool for characterization purposes in the field of chiroptics. Nevertheless, it illustrates a fundamental interplay between molecular and magnetic field symmetries, giving access to information on molecular high order susceptibilities not involved in other linear and nonlinear chiroptical spectroscopies. It is on the other hand worth mentioning that oriented chiral assemblies should in principle show SHG due to magnetic alignment, and there the effect might be stronger than estimated for our contribution, which arises in isotropic samples due to electronic rearrangements.

Macroscopic orientation of the sample could therefore strongly enhance the MFISHG chiroptical effect.

## Appendix: twisted frozen hydrogen peroxide

Table 5 allows to analyze the dependence of third order susceptibility $\chi'^{(3)}(-2\omega;\omega,\omega,0)$ on the extension and quality of the basis set for hydrogen peroxide frozen at a geometry where the $\widehat{HOOH}$ angle is of $120°$. Results are shown both for HF-SCF and DFT structural models. It is noted that the effect of electron correlation, as deduced from a comparison of HF-SCF and DFT/B3LYP results, appears to be relevant, with correlation enhancing the response by a factor, rather constant throughout Table 5, of about three. As far as the convergence of the results with the extension and quality of the basis set, double augmentation appears to make a notable difference, with respect to non-augmented or singly augmented sets. Going beyond double augmentation has a much lower effect on the convergence patterns. As far as the cardinal number is concerned, the results pretty close to those obtained with the largest (d-aug-cc-pV5Z) basis set are already obtained at double-zeta level (d-aug-cc-pVDZ results are within 1.5% of those obtained with the d-aug-cc-pV5Z basis set).

Table 6 shows the results obtained using five quite popular density functionals on our frozen twisted hydrogen peroxide. The strong dependence of the results on the choice of the functional is to be noted. BLYP, the functional yielding the largest value of the observable among the set, doubles the value predicted by B3LYP. Cam-B3LYP and BHandHLYP give reasonably close susceptibilities, still three to four times weaker than that predicted by BLYP. The SVWN5 value is about 30% larger than that yielded by B3LYP.

The discussion of the dependence of the results on the choice of the origin of the multipolar expansion, or, to be more precise, on the origin of the magnetic gauge, is based on the

**Table 5** Dependence of the third order susceptibility $\chi'^{(3)}(-2\omega;\omega,\omega,0)$ of twisted hydrogen peroxide on the extension and quality of the basis set, both for HF-SCF and DFT structure models. $\lambda = 1064$ nm

|  | HFSCF | DFT/B3LYP |
|---|---|---|
| aug-cc-pVDZ | 0.0937 | 0.2087 |
| d-aug-cc-pVDZ | 0.1047 | 0.3099 |
| t-aug-cc-pVDZ | 0.1061 | 0.3183 |
| q-aug-cc-pVDZ | 0.1060 | 0.3158 |
| aug-cc-pVTZ | 0.0944 | 0.2442 |
| d-aug-cc-pVTZ | 0.1011 | 0.3049 |
| t-aug-cc-pVTZ | 0.1020 | 0.3088 |
| q-aug-cc-pVTZ | 0.1021 | 0.3109 |
| aug-cc-pVQZ | 0.0987 | 0.2831 |
| d-aug-cc-pVQZ | 0.1015 | 0.3075 |
| t-aug-cc-pVQZ | 0.1013 | 0.3081 |
| q-aug-cc-pVQZ | 0.1013 | 0.3078 |
| aug-cc-pV5Z | 0.1001 | 0.2977 |
| d-aug-cc-pV5Z | 0.1012 | 0.3075 |

**Table 6** The third order susceptibility $\chi'^{(3)}(-2\omega;\omega,\omega,0)$ of twisted hydrogen peroxide computed with the d-aug-cc-pV5Z basis set. $\lambda = 1064$ nm

| System | $\chi'^{(3)}(-2\omega;\omega,\omega,0)/$a.u. |
|---|---|
| B3LYP | 0.3075 |
| BLYP | 0.6325 |
| Cam-B3LYP | 0.2221 |
| BHandHLYP | 0.1629 |
| SVWN5 | 0.4006 |
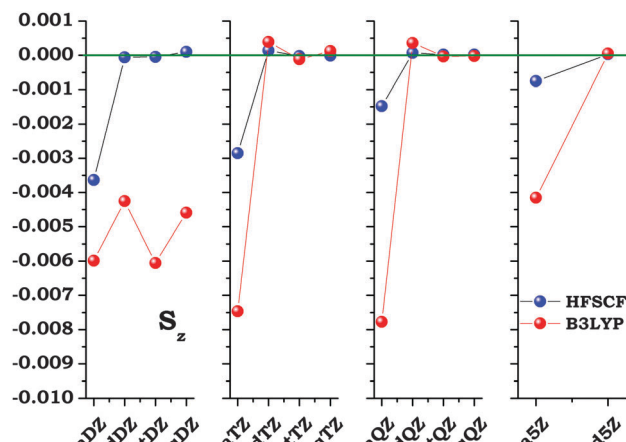


**Fig. 5** The dependence on the extension of the basis set for the **S** vector, containing the molecular contribution to the correction on the third order susceptibility when the origin of the magnetic gauge is displaced for the twisted form of hydrogen peroxide (a.u.). Geometry as shown. See eqn (20) and text for further information.

**Table 7** The dependence on the extension of the basis set for the **S** vector, containing the molecular contribution to the correction on the third order susceptibility when the origin of the magnetic gauge is displaced for the twisted form of hydrogen peroxide ($10^{-3}$ a.u.). Geometry as shown. See eqn (20) and text for further information

|  | HFSCF | DFT/B3LYP |
|---|---|---|
| aug-cc-pVDZ | −3.6353 | −5.9840 |
| d-aug-cc-pVDZ | −0.0593 | −4.2548 |
| t-aug-cc-pVDZ | −0.0477 | −6.0516 |
| q-aug-cc-pVDZ | 0.0975 | −4.5901 |
| aug-cc-pVTZ | −2.8531 | −7.4653 |
| d-aug-cc-pVTZ | 0.1361 | 0.3887 |
| t-aug-cc-pVTZ | −0.0221 | −0.1184 |
| q-aug-cc-pVTZ | −0.0092 | 0.1219 |
| aug-cc-pVQZ | −1.4801 | −7.7739 |
| d-aug-cc-pVQZ | 0.0686 | 0.3579 |
| t-aug-cc-pVQZ | 0.0181 | −0.0368 |
| q-aug-cc-pVQZ | 0.0159 | −0.0241 |
| aug-cc-pV5Z | −0.7542 | −4.1557 |
| d-aug-cc-pV5Z | 0.0285 | −0.0492 |

evidence shown in Fig. 5, see also Table 7. In the limit of a complete one-electron basis set, $S_z$ should vanish, exactly for the HF-SCF case. To start seeing some trend of convergence once again we need to resort at least to doubly augmented correlation consistent sets, although as the cardinal number increases,

**1854** | Phys. Chem. Chem. Phys., 2016, **18**, 1846–1858

This journal is © the Owner Societies 2016

the correction needed when using augmented sets decreases steadily. Once at the doubly augmented level though the correction drops to small values, and yet convergence towards zero is rather slow and not necessarily monotonous. The pattern is even more complicate for B3LYP. Here the hypervirial relationship kicks in more slowly, and it is not safe to speak of convergence towards a vanishing correction $S_z$ within the range of basis sets employed in our analysis.

## Acknowledgements

## References

1 R. W. Boyd, *Nonlinear Optics*, Academic Press, San Diego, 1992.
2 N. Bloembergen, *Nonlinear Optics*, World Scientific, Singapore, 4th edn, 1996.
3 Y. R. Shen, *The Principles Of Nonlinear Optics*, Wiley Classic Library Ed., Wiley Interscience, Hoboken, New Jersey, 2003.
4 G. H. Wagnière, *Linear and Nonlinear Optical Properties of Molecules*, VCH, Basel, 1993.
5 P. N. Butcher and D. Cotter, *The Elements of Nonlinear Optics*, Cambridge Studies in Modern Optics, Cambridge University Press, Cambridge, 1998.
6 M. Göppert-Mayer, Über elementarakte mit zwei quantensprüngen, *Ann. Phys.*, 1931, **9**, 273.
7 W. Kaiser and C. G. B. Garrett, Two-photon excitation in $CaF_2:Eu^{2+}$, *Phys. Rev. Lett.*, 1961, **7**, 229.
8 I. D. Abella, Optical double-quantum absorption in cesium vapor, *Phys. Rev. Lett.*, 1962, **9**, 453.
9 P. Fischer and F. Hache, Nonlinear optical spectroscopy of chiral molecules, *Chirality*, 2005, **17**, 421–437.
10 P. Fischer and B. Champagne, Nonlinear optical properties of chiral liquids: Electric-dipolar pseudoscalars in nonlinear optics, in *Non-Linear Optical Properties of Matter: From molecules to condensed phases, Series: Challenges and Advances in Computational Chemistry and Physics*, ed. M. G. Papadopoulos, J. Leszczynski and A. J. Sadlej, Springer, Dordrecht, The Netherlands, 2006, ch. 12, pp. 359–381.
11 A. Rizzo, S. Coriani and K. Ruud, Response function theory computational approaches to linear and non-linear optical spectroscopy, in *Computational Strategies for Spectroscopy: from Small Molecules to Nano Systems*, ed. V. Barone, John Wiley & Sons, Hoboken, NJ, 2011.
12 G. H. Wagnière, Optical activity of higher order in a medium of randomly oriented molecules, *J. Chem. Phys.*, 1982, **77**, 2786.
13 P. A. Franken, A. E. Hill, C. W. Peters and G. Weinreich, Generation of optical harmonics, *Phys. Rev. Lett.*, 1961, **7**, 118.
14 D. A. Kleinman, Theory of second harmonic generation of light, *Phys. Rev.*, 1962, **128**, 1761.
15 R. Hellwarth and P. Christensen, Nonlinear optical microscope using second harmonic generation, *Appl. Opt.*, 1975, **14**, 247.
16 P. J. Campagnola and L. M. Loew, Second-harmonic imaging microscopy for visualizing biomolecular arrays in cells, tissues and organisms, *Nat. Biotechnol.*, 2003, **21**, 1356.
17 T. Boulesteix, E. Beaurepaire, M. Sauviat and M. Schanne-Klein, Second-harmonic microscopy of unstained living cardiac myocytes: measurements of sarcomere length with 20-nm accuracy, *Opt. Lett.*, 2004, **29**, 2031.
18 R. M. Williams, W. R. Zipfel and W. W. Webb, Interpreting second-harmonic generation images of collagen I fibrils, *Biophys. J.*, 2005, **88**, 1377.
19 S. V. Plotnikov, A. C. Millard, P. J. Campagnola and W. A. Mohler, Characterization of the myosin-based source for second-harmonic generation from muscle sarcomeres, *Biophys. J.*, 2006, **90**, 693.
20 P. Campagnola, Second harmonic generation imaging microscopy: Applications to diseases diagnostics, *Anal. Chem.*, 2011, **83**, 3224.
21 L. Moreaux, O. Sandre, M. Blanchard-Desce and J. Mertz, Membrane imaging by simultaneous second-harmonic generation and two-photon microscopy, *Opt. Lett.*, 2000, **25**, 320.
22 Y. Chang, H. Wei, Y. Jin, H. Liu and X. Deng, Microscopic second harmonic generation (SHG) from tilt-placed collagen fibrils, *Gen. Physiol. Biophys.*, 2011, **30**, 175.
23 M. Bass, P. A. Franken, A. E. Hill, C. W. Peters and G. Weinreich, Optical mixing, *Phys. Rev. Lett.*, 1962, **8**, 18.
24 P. Fischer, K. Beckwitt, F. W. Wise and A. C. Albrecht, The chiral specificity of sum-frequency generation in solutions, *Chem. Phys. Lett.*, 2002, **352**, 463–468.
25 Y. R. Shen, Basic Theory of Surface Sum-Frequency Generation, *J. Phys. Chem. C*, 2012, **116**, 15505–15509.
26 J. E. Laaser, D. R. Skoff, J.-J. Ho, Y. Joo, A. L. Serrano, J. D. Steinkruger, P. Gopalan, S. H. Gellman and M. T. Zanni, Two-dimensional sum-frequency generation reveals structure and dynamics of a surface-bound peptide, *J. Am. Chem. Soc.*, 2014, **136**, 956–962.
27 M. Bass, P. A. Franken, J. F. Ward and G. Weinreich, Optical rectification, *Phys. Rev. Lett.*, 1962, **9**, 442.
28 A. W. Smith and P. Braslau, Optical mixing of coherent and incoherent light, *IBM J. Res. Dev.*, 1962, **6**, 361.
29 C. H. Lee, R. K. Chang and N. Bloembergen, Nonlinear electroreflectance in silicon and silver, *Phys. Rev. Lett.*, 1967, **18**, 167.
30 B. E. A. Saleh and M. C. Teich, in *Fundamentals of Photonics*, ed. J. W. Goodman, Wiley Series in Pure and Applied Optics, John Wiley & Sons, Hoboken, New Jersey, 1991.
31 A. Rizzo and H. Ågren, Ab initio study of the circular intensity difference in electric-field-induced second harmonic generation of chiral natural amino acids, *Phys. Chem. Chem. Phys.*, 2013, **15**, 1198–1207.
32 Y. T. Lam and T. Thirunamachandran, Direct current-induced second harmonic generation by chiral molecules, *J. Chem. Phys.*, 1982, **77**, 3810.

This journal is © the Owner Societies 2016

*Phys. Chem. Chem. Phys.*, 2016, **18**, 1846–1858 | **1855**

33 D. P. Craig and T. Thirunamachandran, *Molecular Quantum Electrodynamics. An Introduction to Radiation Molecule Interaction*, Dover Publications, Inc., Mineaol, New York, 1984.

34 E. U. Condon, Theories of Optical Rotatory Power, *Rev. Mod. Phys.*, 1937, **9**, 432.

35 D. J. Cadwell and H. Eyring, *The Theory of Optical Activity*, Wiley-Interscience, New York, 1971.

36 L. D. Barron, *Molecular light scattering and optical activity*, Cambridge University Press, Cambridge, 2004.

37 K. Nakanishi, N. Berova and R. W. Woody, *Circular dichroism: principles and applications*, VCH Publishers Inc., New York, 1994.

38 M. Matsuoka, H. Nakatsuka, H. Uchiki and M. Mitsunaga, Optical Second-Harmonic Generation in Gases: *Rotation* of Quadrupole Moment in Magnetic Field, *Phys. Rev. Lett.*, 1977, **38**, 894.

39 T. Suzuki, V. Venkataramanan and M. Aono, Magnetic-field-induced optical second-harmonic generation on Si(111)-7 × 7, *Jpn. J. Appl. Phys.*, 2001, **40**, L1119.

40 V. V. Pavlov, A. M. Kalashnikova, R. V. Pisarev, I. Sänger, D. R. Yakovlev and M. Bayer, Magnetic-Field-Induced Optical Second-Harmonic Generation in Semiconductor GaAs, *Phys. Rev. Lett.*, 2005, **94**, 157404.

41 R. V. Pisarev, I. Sänger, G. A. Petrakovskii and M. Fiebig, Magnetic-Field-Induced Optical Second-Harmonic Generation in $CuB_2O_4$, *Phys. Rev. Lett.*, 2004, **93**, 037204.

42 O. A. Aktsipetrov, T. V. Murzina, E. M. Kim, R. V. Kapra, A. A. Fedyanin, M. Inoue, A. F. Kravets, S. V. Kuznetsova, M. V. Ivanchenko and V. G. Lifshits, Magnetization-induced second- and third-harmonic generation in magnetic thin films and nanoparticles, *J. Opt. Soc. Am. B*, 2005, **22**, 138.

43 T. Rasing and H. A. Wierenga, Magnetic-field-induced second-harmonic generation, *Ferroelectrics*, 1994, **162**, 217.

44 S. Kielich and R. Zawodny, DC magnetic field-induced second harmonic generation of laser beam, *Opt. Commun.*, 1971, **4**, 132.

45 N. L. Manakov, S. I. Marmo and V. D. Ovsiannikov, Magnetic-field-induced optical second-harmonic generation, *Laser Phys.*, 1995, **5**, 181.

46 A. Kirilyuk and T. Rasing, Magnetization-induced second harmonic generation, in *Handbook of magnetism and advanced magnetic Materials*, ed. H. Kronmüller and S. Parkin, John Wiley & Sons, Hoboken, NJ, 2007.

47 K. Ikeda, S.-I. Ohkoshi and K. Hashimoto, Magnetization-induced second-harmonic generation in electrochemically synthesized magnetic films of ternary metal prussian blue analogs, *J. Appl. Phys.*, 2003, **93**, 1371.

48 A. A. Fedyanin, T. Yoshida, K. Nishimura, G. Marowsky, M. Inoue and O. A. Aktsipetrov, Magnetization-induced second harmonic generation in magnetophotonic microcavities based on ferrite garnets, *JETP Lett.*, 2002, **76**, 527.

49 H. Y. Hwang, Y. Iwasa, M. Kawasaki, B. Keimer, N. Nagaosa and Y. Tokura, Emergent phenomena at oxide interfaces, *Nat. Mater.*, 2013, **11**, 103.

50 E. Runge and E. K. U. Gross, Density-Functional Theory for Time-Dependent Systems, *Phys. Rev. Lett.*, 1984, **52**, 997.

51 M. A. L. Marques and E. K. U. Gross, Time-dependent density functional theory, *Annu. Rev. Phys. Chem.*, 2004, **55**, 427.

52 R. Ditchfield, Self-consistent perturbation theory of diamagnetism. i. a gauge-invariant LCAO method for NMR chemical shifts, *Mol. Phys.*, 1974, **27**, 789–807.

53 A. J. Thorvaldsen, K. Ruud, A. Rizzo and S. Coriani, Analytical calculations of frequency-dependent hypermagnetizabilities and Cotton-Mouton constants using London Atomic Orbitals, *J. Chem. Phys.*, 2008, **129**, 164110.

54 D. Shcherbin, A. J. Thorvaldsen, D. Jonsson and K. Ruud, Gauge-origin independent calculations of Jones birefringence, *J. Chem. Phys.*, 2011, **135**, 134114.

55 A. J. Thorvaldsen, K. Ruud, K. Kristensen, P. Jørgensen and S. Coriani, A density matrix-based quasienergy formulation of the Kohn-Sham density functional response theory using perturbation- and time-dependent basis sets, *J. Chem. Phys.*, 2011, **129**, 214108.

56 G. L. J. A. Rikken, J. Fölling and P. Wyder, Electrical magnetochiral anisotropy, *Phys. Rev. Lett.*, 2001, **87**, 236602.

57 V. Krstić, S. Roth, M. Burghard, K. Kern and G. L. J. A. Rikken, Magneto-chiral anisotropy in charge transport through single-walled carbon nanotubes, *J. Chem. Phys.*, 2002, **117**, 11315.

58 V. Krstić and G. L. J. A. Rikken, Magneto-chiral anisotropy of the free electron on a helix, *Chem. Phys. Lett.*, 2002, **364**, 51.

59 F. Pop, P. Auban-Senzier, E. Canadell, G. L. J. A. Rikken and N. Avarvari, Electrical magnetochiral anisotropy in a bulk chiral molecular conductor, *Nat. Commun.*, 2001, **87**, 236602.

60 D. L. Andrews and T. Thirunamachandran, On three dimensional rotational averages, *J. Chem. Phys.*, 1977, **67**, 5026.

61 R. R. Birss, Macroscopic symmetry in space-time, *Rep. Prog. Phys.*, 1963, **26**, 307.

62 B. J. Orr and J. F. Ward, Perturbation theory of the nonlinear optical polarization of an isolated system, *Mol. Phys.*, 1971, **20**, 513–526.

63 J. Olsen and P. Jørgensen, Linear and nonlinear response functions for an exact state and for an MCSCF state, *J. Chem. Phys.*, 1985, **82**, 3235.

64 J. Olsen and P. Jørgensen, Time-dependent response theory with applications to self-consistent field and multiconfigurational self-consistent field wave functions, in *Modern Electronic Structure Theory*, ed. D. R. Yarkony, World Scientific, 1995, vol. 2.

65 P. Norman, D. Jonsson, O. Vahtras and H. Ågren, Nonlinear electric and magnetic properties obtained from cubic response functions in the random phase approximation, *Chem. Phys.*, 1996, **203**, 23.

66 D. Jonsson, P. Norman and H. Ågren, Cubic response functions in the multiconfiguration self-consistent field approximation, *J. Chem. Phys.*, 1996, **105**, 6401.

67 C. Hättig, O. Christiansen and P. Jørgensen, Frequency-dependent second hyperpolarizabilities using coupled cluster cubic response theory, *Chem. Phys. Lett.*, 1998, **282**, 139.

68 P. Saeek, D. Jonsson, O. Vahtras and H. Ågren, Density-functional theory of linear and nonlinear time-dependent molecular properties, *J. Chem. Phys.*, 2002, **117**, 9630.

69 B. Jansík, P. Saeek, D. Jonsson, O. Vahtras and H. Ågren, Cubic response functions in time-dependent density functional theory, *J. Chem. Phys.*, 2005, **122**, 054107.

70 A. D. Becke, Density-functional thermochemistry. III. The role of exact exchange, *J. Chem. Phys.*, 1993, **98**, 5648.

71 A. D. Becke, Density-functional exchange-energy approximation with correct asymptotic behavior, *Phys. Rev. A: At., Mol., Opt. Phys.*, 1988, **38**, 3098.

72 C. Lee, W. Yang and R. G. Parr, Development of the Colle-Salvetti correlation-energy formula into a functional of the electron density, *Phys. Rev. B: Condens. Matter Mater. Phys.*, 1988, **37**, 785.

73 W. J. Hehre, R. Ditchfield and J. A. Pople, Self-Consistent Molecular Orbital Methods. XII. Further Extensions of Gaussian-Type Basis Sets for Use in Molecular Orbital Studies of Organic Molecules, *J. Chem. Phys.*, 1972, **56**, 2257.

74 N. Lin, F. Santoro, X. Zhao, C. Toro, L. D. Boni, F. E. Hernández and A. Rizzo, Computational challenges in simulating and analyzing experimental linear and non-linear circular dichroism spectra. R-(+)-1,1′-bi(2-naphtol) as a prototype case, *J. Phys. Chem. B*, 2011, **115**, 811–824.

75 R. Sahnoun, S. Koseki and Y. Fujimura, Theoretical investigation of 1,1′-bi-2-naphthol isomerization, *J. Mol. Struct.*, 2005, **735–736**, 315–324.

76 R. Ditchfield, W. J. Hehre and J. A. Pople, Self-Consistent Molecular-Orbital Methods. IX. An Extended Gaussian-Type Basis for Molecular-Orbital Studies of Organic Molecules, *J. Chem. Phys.*, 1971, **54**, 724–728.

77 B. Jansík, A. Rizzo, H. Ågren and B. Champagne, Strong two-photon circular dichroism in helicenes: a theoretical investigation, *J. Chem. Theory Comput.*, 2008, **4**, 457.

78 T. H. Dunning, Gaussian-basis sets for use in correlated molecular calculations. 1. The atoms boron through neon and hydrogen, *J. Chem. Phys.*, 1989, **90**, 1007–1023.

79 R. A. Kendall, T. H. Dunning and R. J. Harrison, Electron-affinities of the 1st-row atoms revisited – systematic basis-sets and wave-functions, *J. Chem. Phys.*, 1992, **96**, 6796–6806.

80 M. J. Frisch, G. W. Trucks, H. B. Schlegel, G. E. Scuseria, M. A. Robb, J. R. Cheeseman, J. A. Montgomery, Jr., T. Vreven, K. N. Kudin, J. C. Burant, J. M. Millam, S. S. Iyengar, J. Tomasi, V. Barone, B. Mennucci, M. Cossi, G. Scalmani, N. Rega, G. A. Petersson, H. Nakatsuji, M. Hada, M. Ehara, K. Toyota, R. Fukuda, J. Hasegawa, M. Ishida, T. Nakajima, Y. Honda, O. Kitao, H. Nakai, M. Klene, X. Li, J. E. Knox, H. P. Hratchian, J. B. Cross, C. Adamo, J. Jaramillo, R. Gomperts, R. E. Stratmann, O. Yazyev, A. J. Austin, R. Cammi, C. Pomelli, J. W. Ochterski, P. Y. Ayala, K. Morokuma, G. A. Voth,

P. Salvador, J. J. Dannenberg, V. G. Zakrzewski, S. Dapprich, A. D. Daniels, M. C. Strain, O. Farkas, D. K. Malick, A. D. Rabuck, K. Raghavachari, J. B. Foresman, J. V. Ortiz, Q. Cui, A. G. Baboul, S. Clifford, J. Cioslowski, B. B. Stefanov, G. Liu, A. Liashenko, P. Piskorz, I. Komaromi, R. L. Martin, D. J. Fox, T. Keith, M. A. Al-Laham, C. Y. Peng, A. Nanayakkara, M. Challacombe, P. M. W. Gill, B. Johnson, W. Chen, M. W. Wong, C. Gonzalez and J. A. Pople, *Gaussian 03, Revision A.1*, Gaussian, Inc., Pittsburgh, PA, 2003.

81 Dalton, a molecular electronic structure program, Release 2.0, 2005, see http://www.kjemi.uio.no/software/dalton/dalton.html.

82 K. Aidas, C. Angeli, K. L. Bak, V. Bakken, R. Bast, L. Boman, O. Christiansen, R. Cimiraglia, S. Coriani, P. Dahle, E. K. Dalskov, U. Ekström, T. Enevoldsen, J. J. Eriksen, P. Ettenhuber, B. Fernández, L. Ferrighi, H. Fliegl, L. Frediani, K. Hald, A. Halkier, C. Hättig, H. Heiberg, T. Helgaker, A. C. Hennum, H. Hettema, E. Hjertenæs, S. Høst, I.-M. Høyvik, M. F. Iozzi, B. Jansík, H. J. A. Jensen, D. Jonsson, P. Jørgensen, J. Kauczor, S. Kirpekar, T. Kjærgaard, W. Klopper, S. Knecht, R. Kobayashi, H. Koch, J. Kongsted, A. Krapp, K. Kristensen, A. Ligabue, O. B. Lutnæs, J. I. Melo, K. V. Mikkelsen, R. H. Myhre, C. Neiss, C. B. Nielsen, P. Norman, J. Olsen, J. M. H. Olsen, A. Osted, M. J. Packer, F. Pawlowski, T. B. Pedersen, P. F. Provasi, S. Reine, Z. Rinkevicius, T. A. Ruden, K. Ruud, V. Rybkin, P. Salek, C. C. M. Samson, A. S. de Merás, T. Saue, S. P. A. Sauer, B. Schimmelpfennig, K. Sneskov, A. H. Steindal, K. O. Sylvester-Hvid, P. R. Taylor, A. M. Teale, E. I. Tellgren, D. P. Tew, A. J. Thorvaldsen, L. Thøgersen, O. Vahtras, M. A. Watson, D. J. D. Wilson, M. Ziolkowski and H. Ågren, The Dalton quantum chemistry program system, *Wiley Interdiscip. Rev.: Comput. Mol. Sci.*, 2014, 269–284.

83 A. Rizzo, B. Jansík, T. Bondo Pedersen and H. Ågren, Origin independent approaches to the calculation of two-photon circular dichroism, *J. Chem. Phys.*, 2006, **125**, 064113.

84 B. Miehlich, A. Savin, H. Stoll and H. Preuss, Results obtained with the correlation-energy density functionals of Becke and Lee, Yang and Parr, *Chem. Phys. Lett.*, 1989, **157**, 200.

85 A. D. Becke, A new mixing of Hartree–Fock and local density-functional theories, *J. Chem. Phys.*, 1993, **98**, 1372.

86 Y. Yanai, D. P. Tew and N. C. Handy, A new hybrid exchange–correlation functional using the Coulomb-attenuating method (CAM-B3LYP), *Chem. Phys. Lett.*, 2004, **393**, 51.

87 M. J. G. Peach, T. Helgaker, P. Saeek, T. W. Keal, O. B. Lutnæs, D. J. Tozer and N. C. Handy, Assessment of a Coulomb-attenuated exchange–correlation energy functional, *Phys. Chem. Chem. Phys.*, 2006, **8**, 558.

88 M. J. Paterson, O. Christiansen, F. Pawoowski, P. Jørgensen, C. Hättig, T. Helgaker and P. Saeek, Benchmarking two-photon absorption with CC3 quadratic response theory and comparison with density functional response theory, *J. Chem. Phys.*, 2006, **124**, 054322.

This journal is © the Owner Societies 2016

*Phys. Chem. Chem. Phys.*, 2016, **18**, 1846–1858 | 1857

89 S. H. Vosko, L. Wilk and M. Nusair, Accurate spin-dependent electron liquid correlation energies for local spin density calculations: A critical analysis, *Can. J. Phys.*, 1980, **58**, 1200–1211.

90 J. C. Slater, *The Self-Consistent Field for Molecular and Solids, Quantum Theory of Molecular and Solids*, McGraw-Hill, New York, 1974, vol. 4.

91 A. Osted, J. Kongsted and O. Christiansen, Theoretical study of the electronic gas-phase spectrum of glycine, alanine and related amines and carboxylic acids, *J. Phys. Chem. A*, 2005, **109**, 1430.

92 G. Pescitelli, L. Di Bari and N. Berova, Conformational aspects in the studies of organic compounds by electronic circular dichroism, *Chem. Soc. Rev.*, 2011, **40**, 4604–4625.

93 C. Toro, L. De Boni, N. Lin, F. Santoro, A. Rizzo and F. E. Hernandez, Two-photon absorption circular dichroism: a new twist in nonlinear spectroscopy, *Chemistry*, 2010, **16**, 3504–3509.

94 P. Norman, D. Bishop, H. Jensen and J. Oddershede, Near-resonant absorption in the time-dependent self-consistent field and multiconfigurational self-consistent field approximations, *J. Chem. Phys.*, 2001, **115**, 10323.

95 P. Norman, A perspective on nonresonant and resonant electronic response theory for time-dependent molecular properties, *Phys. Chem. Chem. Phys.*, 2011, **13**, 20519.

96 K. Kristensen, J. Kauczor, T. Kjærgaard and P. Jørgensen, A perspective on nonresonant and resonant electronic response theory for time-dependent molecular properties, *J. Chem. Phys.*, 2009, **131**, 044112.

97 K. Kristensen, J. Kauczor, A. J. Thorvaldsen, P. Jørgensen, T. Kjærgaard and A. Rizzo, Damped response theory description of two-photon absorption, *J. Chem. Phys.*, 2011, **134**, 214104.

98 E. R. Cohen, T. Cvita, J. G. Frey, B. Holmström, K. Kuchitsu, R. Marquardt, I. Mills, F. Pavese, M. Quack, J. Stohner, H. L. Strauss, M. Takami and A. J. Thor, *Quantities, Units and Symbols in Physical Chemistry*, IUPAC, RCS Publishing, Mineaol, New York, 3rd edn, 2007.

99 D. N. Nikogosyan and G. G. Gurzadyan, Crystals for nonlinear optics. Biaxial crystals, *Sov. J. Quantum Electron.*, 1987, **17**, 970–977.

100 B. Albertazzi, J. Béard, A. Ciardi, T. Vinci, J. Albrecht, J. Billette, T. Burris-Mog, S. N. Chen, D. Da Silva, S. Dittrich, T. Herrmannsdörfer, B. Hirardin, F. Kroll, M. Nakatsutsumi, S. Nitsche, C. Riconda, L. Romagnagni, H.-P. Schlenvoigt, S. Simond, E. Veuillot, T. E. Cowan, O. Portugall, H. Pépin and J. Fuchs, Production of large volume, strongly magnetized laser-produced plasmas by use of pulsed external magnetic fields, *Rev. Sci. Instrum.*, 2013, **84**, 043505.

101 A. Capobianco, R. Centore, S. Fusco and A. Peluso, Electro-optical properties from cc2 calculations: A comparison between theoretical and experimental results, *Chem. Phys. Lett.*, 2013, **580**, 126–129.